frontiers in Energy Research

ORIGINAL RESEARCH
published: 07 September 2020
doi: 10.3389/fenrg.2020.00197

Study on the Breakdown Mechanism of Water Film on Corrugated Plate Wall Under the Horizontal Shear of Airflow: A Short Communication

Bo Wang[1], Bowen Chen[1], Bingzheng Ke[1], Gongqing Wang[1], Ru Li[1], Jiming Wen[1], Chuan Lu[2] and Ruifeng Tian[1]**

[1] *Fundamental Science on Nuclear Safety and Simulation Technology Laboratory, Harbin Engineering University, Harbin, China,* [2] *Science and Technology on Reactor System Design Technology Laboratory, Nuclear Power Institute of China, Chengdu, China*

OPEN ACCESS

Edited by:
Shripad T. Revankar, Purdue University, United States

Reviewed by:
Subash Sharma, University of Massachusetts Lowell, United States
Mingjun Wang, Xi'an Jiaotong University, China

***Correspondence:**
Bo Wang
bowang@hrbeu.edu.cn
Ruifeng Tian
ruifengtian@hrbeu.edu.cn

Specialty section:
This article was submitted to Nuclear Energy, a section of the journal Frontiers in Energy Research

Received: *05 June 2020*
Accepted: *27 July 2020*
Published: *07 September 2020*

Citation:
Wang B, Chen B, Ke B, Wang G, Li R, Wen J, Lu C and Tian R (2020) Study on the Breakdown Mechanism of Water Film on Corrugated Plate Wall Under the Horizontal Shear of Airflow: A Short Communication. Front. Energy Res. 8:197. doi: 10.3389/fenrg.2020.00197

The corrugated plate dryer (CPD) is an important steam-water separation (SWS) equipment in the steam generator in the secondary loop of nuclear power plants (NPPs). Therefore, it is very important to understand the process and mechanism of liquid film rupture (LFR) on the wall surface of the CPD. In this paper, for the first time, the process of rupture of the liquid film (LF) on the surface of the corrugated plate is studied. The mechanism of LFR on the wall surface of a vertical corrugated plate was studied experimentally. A high-speed camera was used to collect the image of the broken liquid film, and an experimental research on the broken position, the broken process, and the broken shape of the liquid film was carried out. The results show that the rupture of the liquid film on the wall surface of the corrugated plate under the horizontal shear of airflow (HSA) mostly occurs at the upper middle position of the main flow of the liquid film. Also, the rupture position moves up with the increase in the Reynolds number of the liquid film. LFR needs to go through the process of stable flow, single strip-shaped liquid film (SSLF) detachment, two strip-shaped liquid film (TSSLF) formation, and finally chaotic disordered rupture. The angle between the two strip-shaped liquid films (ATSSLF) is positively related to the Reynolds number of the liquid film.

Keywords: nuclear energy, corrugated plate dryer, breakdown mechanism, breakdown position, liquid film, water film rupture process

INTRODUCTION

The corrugated plate dryer (CPD) is an important steam-water separation (SWS) equipment in the steam generator in the secondary loop of nuclear power plants (NPPs; Zhang et al., 2015; Huang et al., 2019; Wang and Tian, 2019a,b,c; Wang et al., 2019; Chen et al., 2020a,b; Fang et al., 2020a,b; Wang et al., 2020a,b,c). Therefore, it is very important to understand the process and mechanism of liquid film rupture (LFR) on the wall surface of the CPD. The structural

diagram of the CPD and the distribution of airflow and LF inside the CPD are shown in **Figure 1**.

The LFR due to the horizontal shear of airflow (HSA) has a great influence on the gas–water separation effect of the CPD. As the HSA increases, the stable LF will rupture at a certain instant. The separation mechanism of the LFR is also closely related to the position of the LFR and the movement behavior after the rupture. Zhang et al. (2015) studied the fluctuation of the LF on the wall surface of the CPD. Wang and Tian studied the rupture characteristics of the LF on the surface of the CPD (Wang et al., 2019; Wang and Tian, 2019a,b,c; Wang et al., 2020c). Chen et al. (2020a; 2020b) studied the motion behavior of droplets in the CPD. For the current research status of the LF on CPD, refer to reference (Wang et al., 2019). This article will not repeat them here.

The above studies mainly focused on the study of the volatility of the liquid film and the separation efficiency of the CPD. The current research shows that there is no characteristic frequency for the volatility of the liquid film on CPD wall. When the Reynolds number is small enough, the gravity of the LF will not cause the LF to break. Therefore, based on this, many scholars simplified complex three-dimensional problems into two-dimensional models when studying LFR. Nonetheless, due to the complexity of the LFR process, research on the LFR and morphology under HSA has not been unified. There is not enough research on the phenomenon of two strip-shaped liquid film (TSSLF) accompanied by large airflow velocity. In this paper, the LF on the wall surface of the CPD under the HSA is taken as a research object to study the shape and process of LFR.

EXPERIMENT ON LFR

An LFR experiment was conducted on a corrugated plate with a plate spacing of 18.2 mm, height of 250 mm, and folding angle of 33 degrees. The schematic diagram of the experimental bench can refer to reference (Wang et al., 2020c), because this article uses the same experimental bench as reference (Wang et al., 2020c). However, the parameters of CPD applied for the article and reference (Wang et al., 2020c) are different. Similarly, the capture of LF and measurement of PLIF can be seen in reference (Wang et al., 2020c). The parameters of the CPD selected in the article are much smaller than those applied in NPPs. This is because these CPD parameters may contribute to small NPPS such as nuclear power ships.

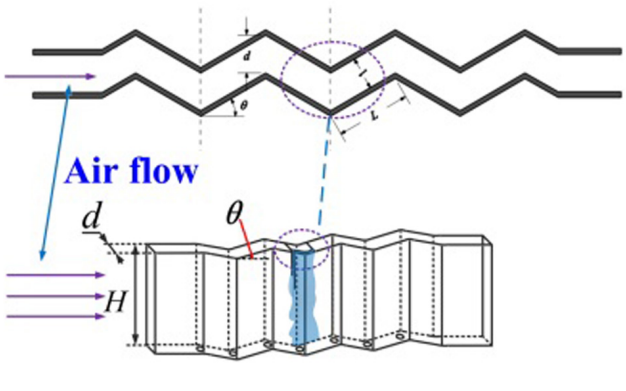

FIGURE 1 | Structure of the corrugated plate and the distribution of different phases in the corrugated plate dryer (CPD).

The LF with Rhodamine B fluorescent stain with a maximum absorption wavelength of 555 nm flows from the high-level water tank to the stabilized water tank (Wang et al., 2020c). The level of height of the liquid on the left side of the stabilized water tank will not change, and the excess liquid will flow into the tank, which makes the LF pressure unchanged. The liquid film generated by the LF generator flows stably and uniformly down the wall. The LF flowing through the experiment section flows from the drain water tank at the CPD bottom to collection tank and enters the circulating water tank. In this study, a slit method is applied for the generation of a thin LF, that is, a horizontal slit is set on CPD so that the LF flows smoothly on the wall (Wang and Tian, 2019a). The air flowing from the blower passes through the stable section and enters the experimental section area. In the experiment, the airflow speed was gradually increased. When the LF just broke, it was observed that small droplets flew out from the LF mainstream surface, that is, the LF was considered to have broken. Specific details can be found in reference (Wang and Tian, 2019c). For details of the experimental error analysis, image capture method, and PLIF measurement, please refer to the references (Wang and Tian, 2019c; Wang et al., 2020c).

RESULTS AND ANALYSIS

LFR Process

Figure 2 is the image of the liquid film on the wall surface at the corner of the corrugated plate taken by a high-speed camera, which records the rupture process of the liquid film on the wall surface under the HSA. The rupture process when airflow velocity increases from 0 to 7.5 m/s is as follows:

(1) The liquid film flows stably.
(2) The boundary of the liquid film is inclined to the convex angle position of the bending angle of the corrugated plate.
(3) LFR occurs.
(4) Small droplets splash out on the surface of the liquid film mainstream.
(5) Single strip-shaped liquid membranes are detached.
(6) Double strip-shaped liquid film appears.
(7) The mainstream part of the liquid film becomes disordered and ruptures.

The rupture process and morphology of LF under different LF Reynolds numbers are similar (Wang and Tian, 2019b; Wang et al., 2020a,b). LF flows steadily before rupture, and its distribution on the wall surface is very uniform (**Figures 2A,B**). As airflow speed increases, LF distributed at the center of CPD will move to the corner under HSA (**Figures 2C–E**). When it reaches the edge of the CPD corner, due to the surface tension on the solid–liquid interface, the LF will not immediately rupture, but will form a convex arc curve (**Figures 2F,G**). As the airflow

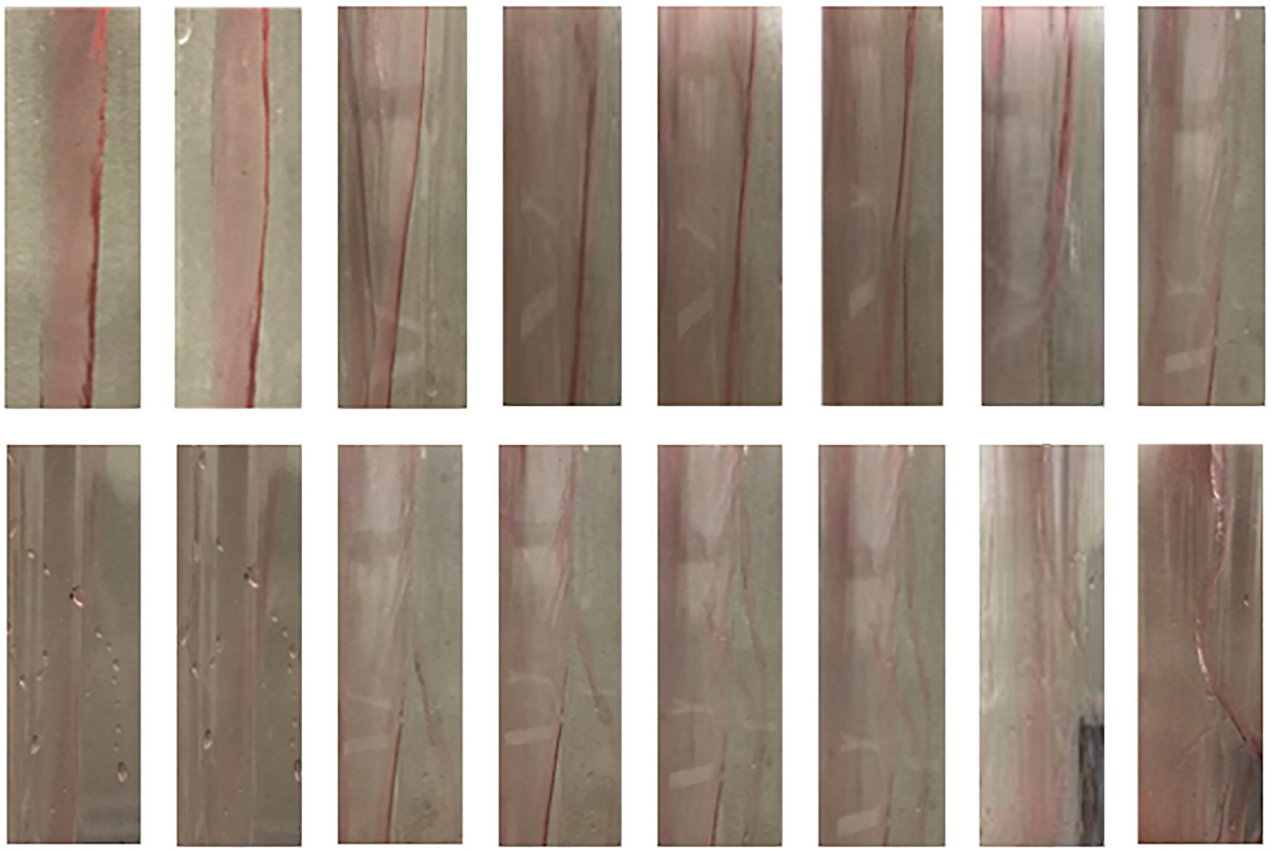

FIGURE 2 | Image of liquid film rupture (LFR) characteristics and process on corrugated plate dryer (CPD) wall.

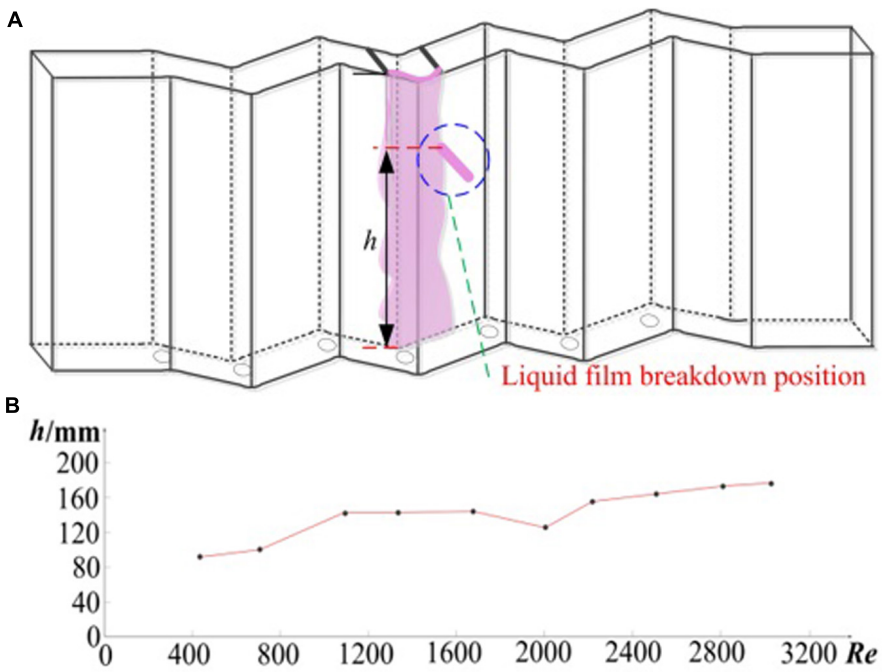

FIGURE 3 | Liquid film rupture (LFR) position. **(A)** Schematic diagram of the LFR position. **(B)** Curve of the LFR position for different *Re*.

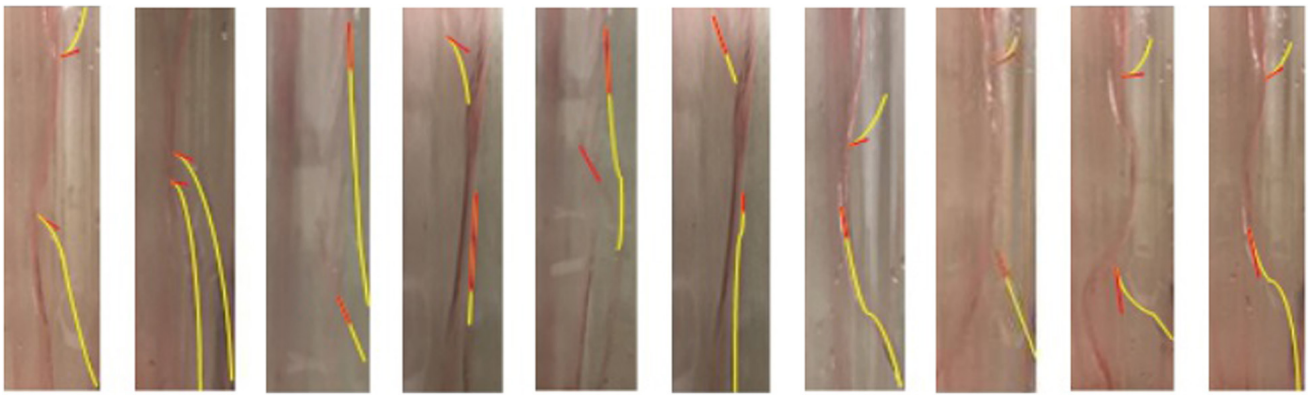

FIGURE 4 | Schematic diagram of two strip-shaped liquid film (TSSLF) for different Reynolds numbers.

rate increases further, LF will suddenly break down at the convex corner of the inflection angle. At the moment of rupture, there will be smaller droplets detached from the LF mainstream. Under the joint action of the gravity of the droplet itself and the airflow, it splashes out in a downward direction, which is the starting moment of the LFR (**Figures 2H–J**). The increase in the airflow rate continuing, the LFR gradually changed from a splash of small droplets to detachment of a single SSLF (**Figures 2K,L**). At this time, due to gravity, the flying distance of the SSLF is significantly reduced compared with the flying distance of small droplets flying away from the LF (because SSLF is heavier than the droplet). As airflow speed gradually increases, the single SSLF gradually develops into the phenomenon of double SSLF splashing. One of the relatively thin strip-shaped liquid films flew away from the surface of the main flow of the liquid film in a horizontal direction or in a downward direction. The other relatively thicker liquid film still maintains the flight direction when the airflow rate is low. Therefore, a certain angle will be formed between the two band-shaped liquid films (**Figures 2M,N**). The increase in the airflow speed kept, most of the LF mainstream cracked. The band-shaped LF disappears, and the shape of the LF when flying away from the LF mainstream has no obvious characteristics (**Figures 2O,P**).

LFR Rupture Position

A schematic diagram of the LFR position and the relationship between LFR position under HSA and *Re* is shown in **Figure 3**.

Most of the LFR occurs in the middle and upper parts of the LF, and the rupture position shows an upward trend with the increase in the Reynolds number of the LF. In the small Reynolds number zone, the rupture position rises faster as the liquid film Reynolds number increases. In the middle Reynolds number zone, the position of the LFR is relatively stable. At high Reynolds numbers, the position of the rupture rises significantly. When the Reynolds number of the LF is large under the same airflow rate, the probability of LFR is relatively high, which will cause the position of the LFR to gradually move up. The phenomenon that the double-strip LF flew away from the wall mainstream LF is due to the fact that when the wind speed is large, an airflow vortex will be formed at the lower part of the LF, causing some LFs to flow back, making the thickness of the upper part of the LF obvious increase (Wang and Tian, 2019a; Wang et al., 2020a). At the same airflow rate, the upper part of the LF is more likely to rupture than the lower half. Therefore, the experiment showed that the LFR mostly occurred in the upper middle part of the mainstream of LF. Moreover, the position of LFR moves up as the Reynolds number increases. In addition, the mass of the reflux of liquid film caused by the vortex is much smaller than the mass of the LF in the lower part of the mainstream; thus, a relatively thin SSLF is formed at the upper part of the LF. The shape of this LF is relatively small, and its gravity is small. It often flew away from the LF surface in a horizontal or slightly downward direction when flying away from the mainstream.

ATSSLF

In the phenomenon of double-strip LF when it ruptures, a certain angle is formed between the flying directions of the TSSLF, that is, the angle between the two strip-shaped liquid films (ATSSLF; as shown in **Figure 4**). The Reynolds numbers of the LF from

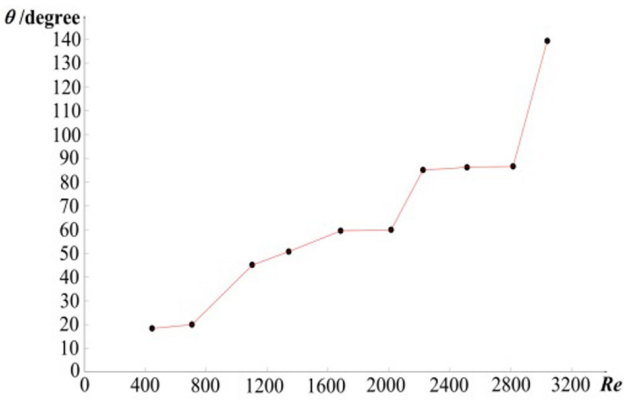

FIGURE 5 | Curve of angle between the two strip-shaped liquid films (ATSSLF) and Reynolds numbers.

left to right are 442.4, 706.2, 1088.7, 1330.0, 1684.9, 2014.1, 2213.1, 2509.0, 2818.6, and 3030.5. The curve of the ATSSLF and Reynolds numbers is shown in **Figure 5**.

It reveals that ATSSLF gradually increased with the increase of *Re*. This is because with the increase in *Re*, the gravity of the thicker one of TSSLFs gradually increases, and the flying distance gradually becomes shorter as it escapes from the LF mainstream. In the experiment, it was found that the flight state of another relatively thin SSLF flying away from the surface of the LF mainstream in the horizontal direction or the downward direction will not change significantly with the Reynolds number. Therefore, the angle of the double-strip liquid film gradually increases with the increase in *Re*. The research on the ATSSLF will still be an important prospect in the future.

CONCLUSION AND PROSPECTS

In this paper, through the experimental study of LFR of the vertical CPD wall under HSA, the following conclusions are drawn.

(1) LFR mostly occurs at the upper middle position of the LF mainstream on the CPD wall surface, and the rupture position generally gradually moves upward as the Reynolds number of the liquid film increases. In the low and high Reynolds numbers, the rupture position increased sharply with the increase in the liquid film Reynolds number. In the middle Reynolds number zone, the position of the rupture did not change significantly.
(2) LFR on the CPD wall surface under HSA passes through the following process.
(a) The LF flows stably.
(b) The LF boundary is inclined to the convex angle position of the CPD dryer.
(c) LFR occurs.
(d) Small droplets splash from the LF mainstream surface.
(e) SSLF is detached.
(f) TSSLF appears.
(g) The mainstream part of the LF becomes disordered and ruptures.
(3) The phenomenon of the TSSLF is caused by the vortex of the airflow generated in the lower part of the experimental section when the airflow rate is large, which causes the upper part of LF to reflux, and the LF is more likely to rupture. Therefore, the angle gradually increases as the Reynolds number of the LF increases. The research on the ATSSLFs will be the prospect research in the future. Nevertheless, due to the difficulty of measurement, our data is relatively small. It is necessary to add experimental data and conduct experiments on CPDs with different parameters in future research. At present, the law of the rupture position of the LF cannot be obtained and unified because the influence of the CPD parameters on the LFR position is great. This is also an important research direction in the future. Many parameters in the LF have non-linear characteristics, which is the future research direction.

DATA AVAILABILITY STATEMENT

The raw data supporting the conclusions of this article will be made available by the authors, without undue reservation.

AUTHOR CONTRIBUTIONS

BW designed this study and mainly performed the experiments. BC, GW, RL, BK, JW, CL, and RT contributed to performing the experiments. BW mainly co-wrote most of the manuscript and all authors contributed to writing the manuscript.

FUNDING

Authors would like to acknowledge the financial support provided by the Ph.D. Student Research and Innovation Fund of the Fundamental Research Funds for the Central Universities (3072020GIP1518), the Fundamental Research Funds for the Central Universities, China Scholarship Council, Chinese Universities Scientific Fund, and the National Natural Science Foundation of China (No. 51676052).

REFERENCES

Chen, B.-W., Wang, B., Mao, F., Tian, R.-F., and Lu, C. (2020a). Analysis of liquid droplet impacting on liquid film by CLSVOF. *Ann. Nuclear Energy* 143:107468. doi: 10.1016/j.anucene.2020.107468

Chen, B.-W., Wang, B., and Tian, R.-F. (2020b). Experimental study of droplet impacting on inclined wetted wall in corrugated plate separator. *Ann. Nuclear Energy* 137:107155. doi: 10.1016/j.anucene.2019.107155

Fang, D., Li, L.-F., Li, J., Wang, M., Yu, H., Zhang, J., et al. (2020a). Full-scale numerical study on the thermal hydraulic characteristics of steam-water separation system in an advanced PWR UTSG. Part two: droplets separation process. *Prog. Nuclear Energy* 118:103139. doi: 10.1016/j.pnucene.2019.103139

Fang, D., Wang, M.-J., Duan, Y.-G., Li, J., Qiu, G., Tian, W., et al. (2020b). Full-scale numerical study on the flow characteristics and mal-distribution phenomena in SG steam-water separation system of an advanced PWR. *Prog. Nuclear Energy* 118:103075. doi: 10.1016/j.pnucene.2019.103075

Huang, Y., Gao, P.-Z., and Wang, C.-Q. (2019). Experimental and numerical investigation of bubble-bubble interactions during the process of free ascension. *Energies* 12, 1–20. doi: 10.3390/en12101977

Wang, B., Chen, B.-W., Ke, B.-Z., Li, R., and Tian, R. (2020a). Study on strip-shaped liquid film in the corrugated plate dryer. *Ann. Nuclear Energy* 139:107237. doi: 10.1016/j.anucene.2019.107237

Wang, B., Chen, B.-W., Wang, G.-Q., Ke, B., Wen, J., Lu, C., et al. (2020b). Analysis of influencing factors of rupture phenomenon of liquid film on the wall of corrugated plate dryer. *Ann. Nuclear Energy* 147:107694. doi: 10.1016/j.anucene.2020.107694

Wang, B., Ke, B.-Z., Chen, B.-W., Li, R., and Tian, R. (2020c). Study on the size of secondary droplets generated owing to rupture of liquid film on corrugated plate wall. *Intern. J. Heat Mass Transf.* 147:118904. doi: 10.1016/j.ijheatmasstransfer.2019.118904

Wang, B., Chen, B.-W., and Tian, R.-F. (2019). Review of research progress on flow and rupture characteristics of liquid film on corrugated plate wall. *Ann. Nuclear Energy* 132, 741–751. doi: 10.1016/j.anucene.2019.06.060

Wang, B., and Tian, R.-F. (2019a). Investigation on flow and breakdown characteristics of water film on vertical corrugated plate wall. *Ann. Nuclear Energy* 127, 120–129. doi: 10.1016/j.anucene.2018.12.001

Wang, B., and Tian, R.-F. (2019b). Judgement of critical state of water film rupture on corrugated plate wall based on SIFT feature selection algorithm and SVM classification method. *Nuclear Eng. Design* 347, 132–139. doi: 10.1016/j.nucengdes.2019.03.025

Wang, B., and Tian, R.-F. (2019c). Study on fluctuation feature and breakdown characteristic of water film on the wall of corrugated plate. *Intern. J. Heat Mass Transf.* 143:118501. doi: 10.1016/j.ijheatmasstransfer.2019.118501

Zhang, H., Liu, Q., Qin, B., and Bo, H. (2015). Simulating particle collision process based on Monte Carlo method. *J. Nucl. Sci. Technol.* 52, 1393–1401. doi: 10.1080/00223131.2014.1003152

Conflict of Interest: The authors declare that the research was conducted in the absence of any commercial or financial relationships that could be construed as a potential conflict of interest.